Assessing the perturbations of the hydrogeological regime in sloping fens through roads

Fabien Cochand[1], Daniel Käser[1], Philippe Grosvernier[2], Daniel Hunkeler[1], Philip Brunner[1]

[1]Centre of Hydrogeology and Geothermics, Université de Neuchâtel, Switzerland.
[2]LIN'eco, ecological engineering, PO Box 51, 2732 Reconvilier, Switzerland.

Corresponding author: Fabien Cochand, fabien.cochand@unine.ch

Abstract

Roads in sloping fens constitute a hydraulic barrier for surface and subsurface flow. This can lead to the drying out of downslope areas of the sloping fen as well as gully erosion. Different types of road construction have been proposed to limit the negative implications of the roads on flow dynamics. However, so far no systematic analysis of their effectiveness has been carried out. This study presents an assessment of the hydrogeological impact of three types of road structures in semi-alpine, sloping fens in Switzerland. Our analysis is based on a combination of field measurements and fully integrated,physically-based modelling. In the field approach, the influence of the road was examined through tracer tests where the upslope of the road was sprinkled with a saline solution. The spatial distribution of electrical conductivity downslope provided a qualitative assessment of the flow paths and thus the implications of the road structures on subsurface flow. A quantitative albeit not site-specific assessment was carried out using numerical models simulating surface and subsurface flow in a fully coupled way. The different road types were implemented in the model and flow dynamics were simulated for a wide range of slopes and hydrogeological conditions such as different hydraulic conductivity of the soil. The results of the field and modelling analysis clearly indicate that roads designed with an L-drain (i.e. collecting water upslope and releasing it in a concentrated manner downslope) constitute the largest perturbations in terms of flow dynamics. The other investigated road structures were found to have less impact. The developed methodologies and results can be used for the planning of future road projects.

1 Introduction

Wetlands can play a significant role in flood control (Baker, 2009;Zollner, 2003;Reckendorfer, 2013), mitigate climate change impacts (Cognard Plancq et al., 2004;Samaritani et al., 2011;Lindsay, 2010;Limpens, 2008) and feature great biodiversity (Rydin, 2005). However, the world has lost 64% of its wetland areas since 1900 and an even greater loss has been observed in Switzerland (Broggi, 1990). Therefore, wetland conservation has received considerable attention. However, the sprawl of human infrastructure, land-use changes, climate change or river regulations remain serious factors that threaten wetlands. For instance, roads can substantially modify the surface-subsurface flow patterns of sloping fens. The changes in flow patterns can influence sediment transport, moisture dynamics and biogeochemical processes as well as ecological dynamics.

The link between hydrological changes and sediment dynamics has been studied in various contexts see e.g. Partington et al. (2017). From a civil engineering perspective, erosion of the road must be avoided. A common strategy to avoid erosion of the road foundation is to collect water in drains and then release it in a concentrated manner downslope. This, however, can lead to erosion of the downslope area, a phenomenon known as « gully erosion ». A number of studies specifically focused on identifying the controlling processes and relevant parameters of gully erosion (Capra et al. (2009);Valentin et al. (2005);Descroix et al. (2008);Poesen et al. (2003);Martínez-Casasnovas (2003);Daba et al. (2003);Betts and DeRose (1999);Derose et al. (1998), among others). Nyssen et al. (2002) investigated the impact of road construction on gully erosion in the northern Ethiopian highlands, with a focus on surface water. In their study area, they observed the formation of a gully after the road construction downslope of the outlets of the drains. Based on fieldwork and subsequent statistical analysis, they concluded that the main causes for gully development are a concentrated runoff, the diversion of concentered runoff to other catchments and the modifications of drainage areas induced by the road. The role of groundwater was not considered in this study.

Reid and Dunne (1984) developed an empirical model for estimating road sediment erosion of roads located in forested catchments in the Washington state (USA). They concluded that a heavily used road produced 130 times more sediment that an abandoned road. Wemple and Jones (2003) also developed an empirical model for estimating runoff production of a forest road at a catchment scale. They demonstrated that during large storm events, subsurface flow can be intercepted by the road. The intercepted water, if directly routed to ditches, increases the rising limb of the catchment hydrograph. At a smaller spatial scale (0.1 km^2) Loague and VanderKwaak (2002) assessed the impact of a road on the surface and subsurface flow using an integrated surface-subsurface flow model

InHM (Integrated Hydrology Model) (VanderKwaak, 1999) in a rural catchment. The results showed that the road induced a slight increase of runoff and a decrease of surface-subsurface water exchange around the road. Dutton et al. (2005) investigated the impact of roads on the near-surface subsurface flow using a variability saturated subsurface model. They concluded that the permeability contrast caused by the road construction leads to a disturbance of near-surface subsurface flow which may significantly modify the physical and ecological environment.

Road construction can also impact the development of vegetation (Chimner, 2016). Von Sengbusch (2015) investigated the changes in the growth of bog pines located in a mountain mire in the black forest (south-west Germany). The author suggests that the increase of bog pine cover is caused by a delayed effect of a road construction in 1983 along a margin of the bog. The road affects the subsurface flow and therefore prevents the upslope water to flow to the bog. According to Von Sengbusch (2015), the road disturbances induce a larger variability in water table elevations during dry periods and consequently increase the sensitivity of the bog to climate change.

Based on these previous studies, a simple conceptual model describing the influence of roads on the flow system can be drawn (Figure 1). In natural conditions, rainwater infiltrates the soil and follows the topographical gradient. In case of heavy precipitation events, water can also directly flow on the surface (runoff in Figure 1a). To construct the foundation of the road, a material with very low permeability is used. This subsequently blocks the flow from the upslope towards the downslope. However, due to the buildup of hydraulic heads in the upslope of the road (Figure 1b), the road can be innundated during precipitation events. To reduce the occurrence of inundations, drains are installed under all roads (Figure 1c). The design and the materials of drains have potentially a significant effect on flow dynamics. Figure 1c presents a typical condition where a non-continuous drain (i.e., drains are perpendicularly installed at regular distances along the road) is installed. The drain captures the flow upslope along the road and the discharge is released in a concentrated manner downslope. This concentration of flow downslope may induce gully erosion and disturb the hydraulic regime of the sloping fens. For example, the wetland is at risk of drying out downslope of the road as the flow is concentrated to a small strip downslope of the drain. Note, however, that a gully must not necessarily develop because the flow-velocity at the drain-exit might not be sufficiently large to trigger erosion. Also, the drying out of the wetland beyond the direct vicinity of the downslope area of the drain must not necessarily happen. The concentrated release from the drain can, to a certain extent, spread out horizontally. In any case, a road constitutes a hydrogeological barrier which perturbs the natural flow dynamics.

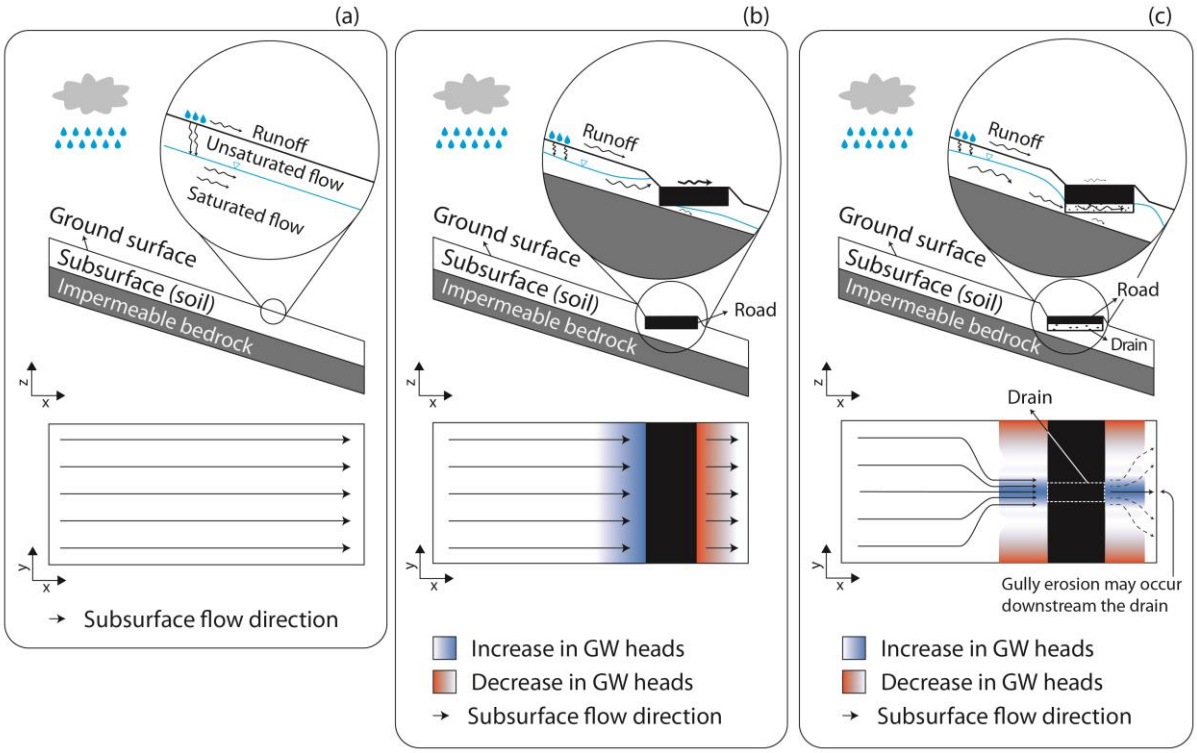

Figure 1: Conceptual subsurface dynamics in sloping fens: a) natural conditions, b) a road without a drain (only shown for illustrative reasons as essentially all roads have drains). In this case, water will flow both across and under the road. Uncontrolled flow beneath the road can cause erosion of the road foundation. c) a road with a drain: In this design, surface water flow is reduced and flow beneath road occurs in a controlled manner through the drain. Water is released downslope in a concentrated manner with the risk of gully erosion and the drying out of parts of the wetland. While it is possible that the concentrated groundwater flows horizontally downslope through natural heterogeneity, there is a high risk of gully erosion.

The design of the roads and especially the drains is expected to have a significant influence on the degree of perturbation. Three fundamentally different road structures were developed in Switzerland to reduce the impacts of roads. These three road types are conceptually illustrated in Figure 2. The efficiency of developed road structures was so far not assessed after completion, neither in the field through field-based experiments, nor on a conceptual level. This study focuses on these three road structures:

- The *no-excavation* structure (Figure 2a) aims at preserving soil continuity under the road. It consists of a leveled layer of gravel, anchored to the ground, and underlying 0.16m thick concrete slabs. Soil compaction is limited by using low-density gravel, made of expanded glass chunks (Misapor™) - approximately fivefold lighter than conventional material.
- The *L-drain* structure (Figure 2b) aims at collecting subsurface water upslope the road and redirecting it to discrete outlets on the other side. The setup consists of a trench, approximately 0.4m deep, filled with a matrix of sandy gravel that contains an L-shaped band of coarse gravel acting as the drain. This is the most common approach to build roads in Switzerland.

- The *wood-log* structure (Figure 2c) aims at promoting homogeneous flow under the road but does not preserve soil continuity. Embedded in a trench, approximately 0.4m deep, the wooden framework is filled with wooden logs forming a permeable medium. The wooden logs are then covered with mixed gravel.

In Switzerland, more than 20'000 ha are included in the national inventory of fens of national importance (Broggi 1990), most of them are located in the mountainous regions of the northern Prealps. These fens developed on nearly impermeable geomorphological layers such as silty moraine material or a particular rock layer named "flysch". The majority of remaining Swiss fens are sloping fens in this particular geological environment. To protect the remaining wetlands it is important to reduce the impact of these constructions, be it in the context of replacing existing, old roads or for the construction of new roads.

The aim of this study is to investigate the hydrogeological impact of the three road structures and their effects on fen water dynamics to support decision-makers in choosing road structures with minimal impact. A combination of fieldwork and hydrogeological modelling tasks was employed. Fieldwork was used to document the hydrogeological impact of existing road structures on fen water dynamics. It is the first time that these road-types are systematically analysed under field conditions. Sites with similar natural conditions were chosen to compare the influence of different road constructions on flow processes. The field studies allow for assessing the effectiveness of a given road structure at a particular location, however, they cannot provide a generalizable analysis of the different road types under different environmental and physical conditions, e.g. the slope or the hydraulic properties of the fen. This gap was filled by the development of generic numerical models. The models are kept deliberately simple in terms of the heterogeneity of the soil. This allows to comparatively explore the potential impact of the different road structures. The modelling allows a systematic comparison of this potential impact for different conditions for the most important hydraulic properties: the slopes of fens and the bulk hydraulic conductivity. However, as the heterogeneity of the soil is not considered in the models and the horizontal redistribution due to field-specific heterogeneity cannot be considered (see figure 1c), the simulations thus constitute a "worst-case " scenario, which allows a ranking the different road structures in terms of perturbation and the risk for gully erosion.

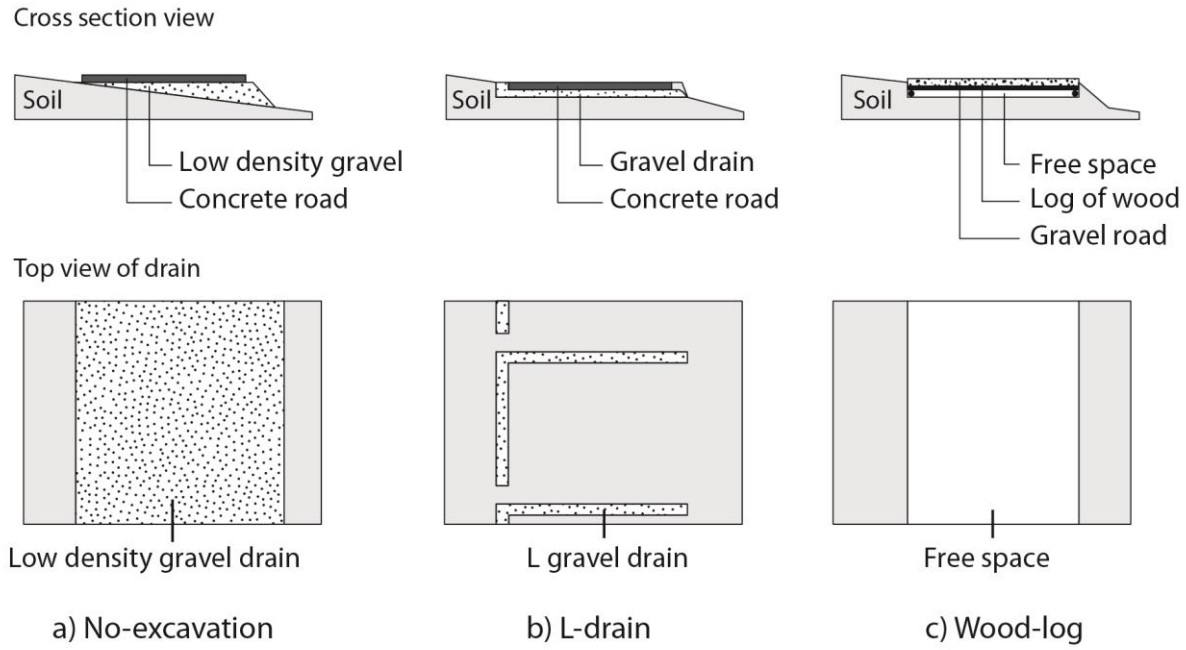

Figure 2 : Conceptual road structures, a) No-excavation road structure, b) L-drain road structure and c) Wood-log road structure.

2 Methods

2.1 Study areas and fieldwork

Four sloping fen areas located in alpine or peri-alpine regions of Switzerland (Table 1) were selected. All areas are situated in protected fen areas, and their selection was based on two main criteria:

1. The subsurface water flow must occur only in the topsoil layer and as runoff (as described in the introduction).
2. The types of installed road structures (no-excavation, L-drain and wood-log).

To fulfil the first criteria, soil profiles were analysed to ensure that each area with different road types had the comparable soil stratigraphy: It had to be composed of organic soil on top of a layer of impermeable clay and similar hydraulic regimes (e.g., runoff and subsurface flow occurring only in the topsoil layer). In addition, to ensure that subsurface water is forced to cross the road instead of flowing in parallel of the road (and thus not being affected directly by the road), another important criterion for the selection of the study areas was that subsurface flow is perpendicular to the road.

To evaluate the hydraulic connection provided by the roadbed structures, tracer tests were carried out. As illustrated schematically in Figure 3, the upslope area was irrigated with a saline solution and the occurrence of

148 the tracer was monitored downslope the road. In the absence of surface runoff, the occurrence of a tracer downslope
149 demonstrates the hydrogeological connection through the road. Furthermore, the spatial distribution of the tracer
150 front reflects the heterogeneity of the flow paths.

151 **Table 1. Field site locations and features.**

	St-Antonien (STA)	**Schoeniseischwand (SCH)**	**Stouffe (STO)**	**Höhmad (HMD)**
Road type	No excavation	L-Drain	Wood-log	Wood-log
Terrain slope	0.27	0.13	0.13	0.15
WGS84 coordinates	46.96760°N 9.84843°E	46.78872°N 7.96805°E	46.72957°N 7.83861°E	46.74027°N 7.89871°E

152

153 On each fieldsite, an area of an 8 x 20m rectangle that includes a 2.5 to 3.5m wide road segment was
154 selected. A network of approximately 30 mini-piezometers on both sides of the road (Figure 3) was installed to
155 monitor the hydraulic heads and was used to obtain samples for the tracer test.

156 The mini-piezometers are high-density polyethene (HDPE) tubes no longer than 1.5m (ID: 24mm). Each
157 tube was screened with 0.4mm slots from the bottom end to 5cm below ground level. It was inserted into the soil
158 after extracting a core with a manual auger (diameter: 4-6cm). The gap between the tube and the soil was filled
159 with fine gravel and sealed on the top with a 4cm thick layer of bentonite or local clay. Hydraulic heads were
160 measured using a manual water-level meter (± 0.3cm). At each point, the terrain and the top of the piezometer
161 were levelled using a level (± 0.3cm), whereas the horizontal position was measured with a tape measure (± 5cm).

162 The tracer tests were conducted using two oscillating sprinklers designed to reproduce a 30mm rain event
163 during 2-3 hours. This is equivalent to an intense rain event. Prior to the experiment, the sprinklers were activated
164 for 15-60 minutes to wet the soil surface. Sodium chloride was added to the irrigated solution to obtain an electrical
165 conductivity of 5-10mS/cm which is approximately ten times higher than the natural electrical conductivity of the
166 groundwater. Subsequently, the area (60m^2) upslope of the road (upslope injection area of Figure 3) was irrigated
167 with the salt solution using the two sprinklers. The electrical conductivity (EC) of soil water was manually
168 measured using a conductivity meter in all mini-piezometers prior to the experiment, immediately after, and 24h
169 later. An increase in EC in piezometers located in the downslope area indicates that the injected salt water flowed
170 from the upslope area to the downslope area below the road and clearly shows a hydraulic connection. Conversely,
171 if no changes in EC are observed in piezometers, this indicates a strongly hampered hydraulic connection below
172 the road.

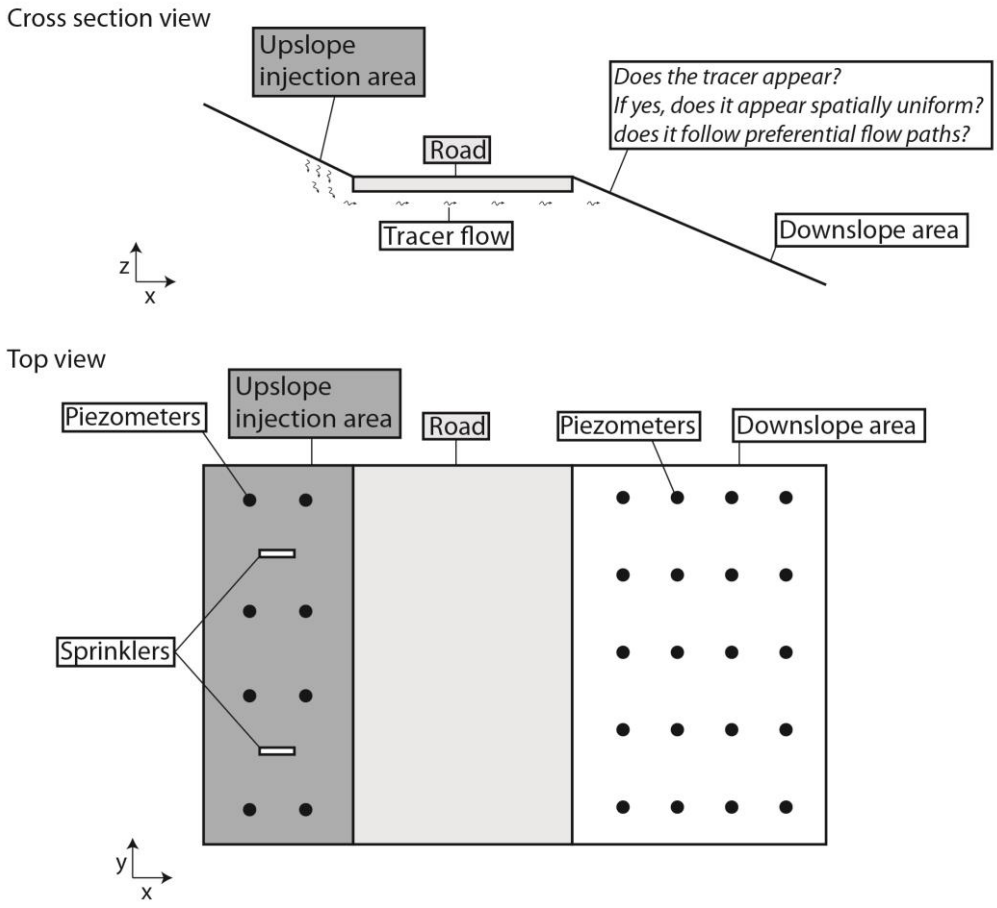

Figure 3 : Schematic view of the fieldwork areas.

2.2 Numerical modelling

The modelling approach was structured in three steps. First, a 3D base case model representing surface and subsurface water flow in a sloping fen was elaborated. Subsequently, the base case model was modified to represent the three different types of road structures. For each model, various slopes, soil and road drain hydraulic conductivities were implemented to produce a sensitivity analysis and explore their sensitivities in the sloping fen flow dynamics (see section 2.2.3 for details).

2.2.1 Numerical simulator

The model used in the study is HydroGeoSphere (HGS) (Aquanty, 2017). HGS is a physically-based surface–subsurface fully-integrated model using the control volume finite element approach. HGS solves a modified Richards' equation describing the 3D subsurface flow. If the subsurface flow is unsaturated, HGS employs the Van Genuchten (1980) functions to relate pressure head to saturation and relative hydraulic conductivity. Simultaneously, HGS solves the 2D depth-averaged diffusion-wave approximation of the Saint-Venant equation for describing the surface flow. To couple surface and subsurface and simulate the water exchanges between both domains, the "dual node approach" is used. In this approach, the top nodes representing the ground surface are

used for calculating both subsurface and surface flow, the exchange flux between the two domains is calculated on the basis of the head-difference between the surface and the subsurface and a coupling factor.

The iterative Newton-Raphson method is used to solve the nonlinear equations. At each subsurface node, saturation and groundwater heads are calculated, which allows for the calculation of the Darcy flux. For further details on the code, HGS capabilities and application, see Aquanty (2017), Brunner and Simmons (2012) or Cochand et al. (2019).

2.2.2 Conceptual models and model implementation

Figure 4 illustrates the conceptual model of each case. Existing engineering sketches were used as a basis for the implementation of the drain and road. Geometry, topography, and slopes are based on the conditions in the field. In each model, the soil layer has a thickness of 0.4m and the surface and subsurface water is only supplied by precipitation. The upslope boundary is the catchment boundary (water divide) and the downslope boundary represents the outlet of the model. Finally, it was assumed that the layer beneath the soil was impermeable (as observed in the field). One Neumann (constant flux) boundary condition was used on the top face for simulating precipitation. A constant head boundary condition (Dirichlet type) equal to the ground surface elevation (2m) was used on the lowest cells of the slope (x=76m on the Figure 5a) allowing groundwater to flow out of the model. Finally, a critical depth boundary condition which allows surface water to flow out of the model domain was implemented on the top nodes located at x=76m. All other faces are no-flow boundary conditions.

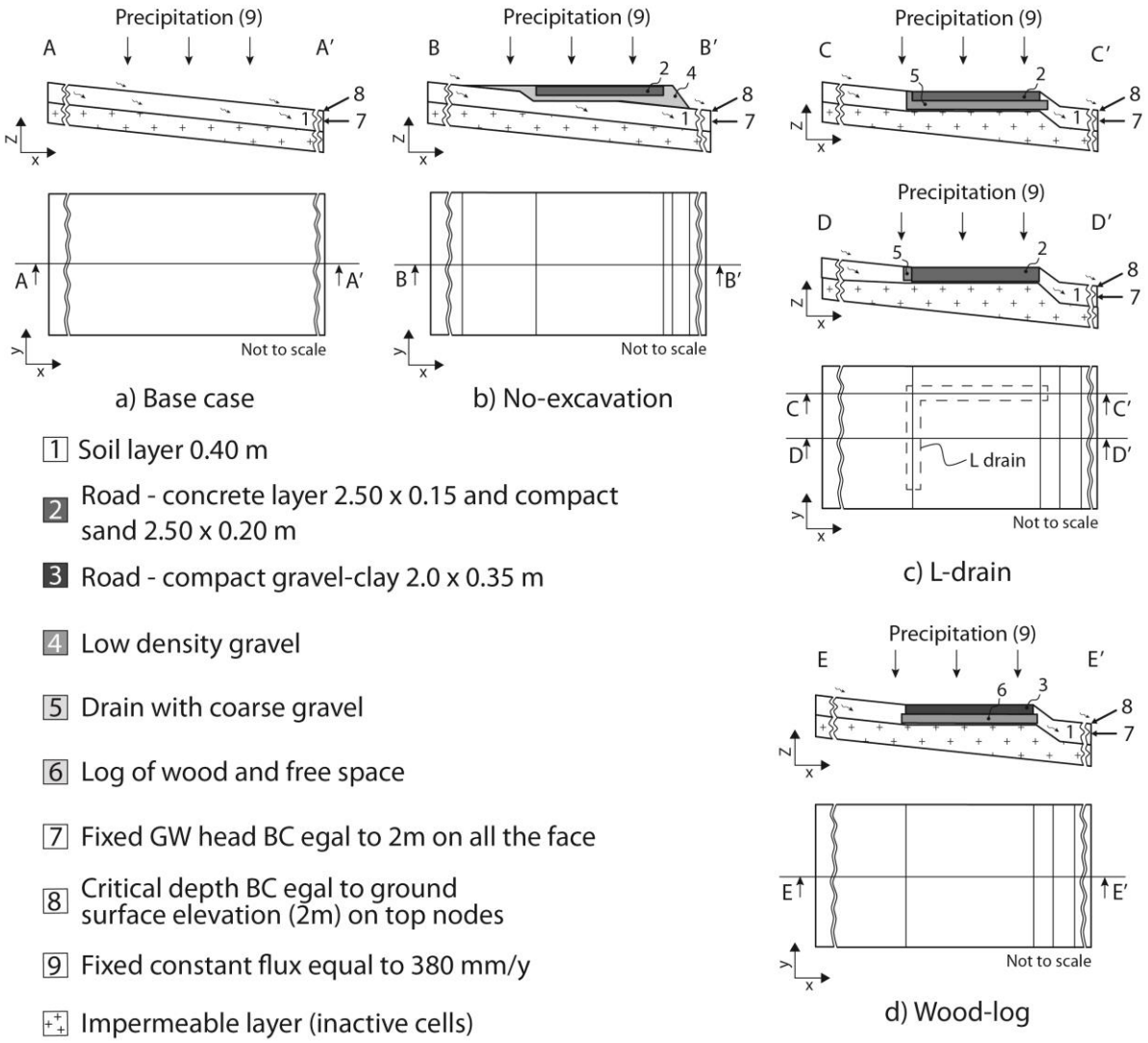

206

207 **Figure 4 : a) Base case, b) No-excavation, c) L-drain and d) Wood-log structures conceptual models.**

208 A 3D- finite element mesh was developed (Figure 5a). The mesh is 76m long in the X direction, 20m in the
209 Y direction and the mesh thickness is 1.2m. The top elevation was fixed at 2m on the right side (x=76m) and varies
210 from 9.6m to 24.8m on the left side (x=0) according to the slope of the model. The mesh was composed of 24
211 layers, 127,200 nodes and 118,440 rectangular prism elements. To guarantee numerical stability, mesh refinements
212 were implemented. The element size varies between 2m and 0.1m horizontally (in the X and Y directions) and
213 0.09m and 0.06m vertically.

214 The base case model and the three other models representing different road types have the same boundary
215 conditions and finite element meshes, however, modifications were made between coordinates 61<x<66 for the
216 implementation of the different road types. Figure 5 depicts the differences between the base case model (Figure
217 5a and b) and models with roads (Figure 5c, d, e and f). In models simulating a road, the mesh and the material

properties were adjusted. The fine spatial discretization of the mesh created between the coordinates 61<x<66 allows a more accurate representation of the simulated processes where high hydraulic gradients are expected (near roads and drains).

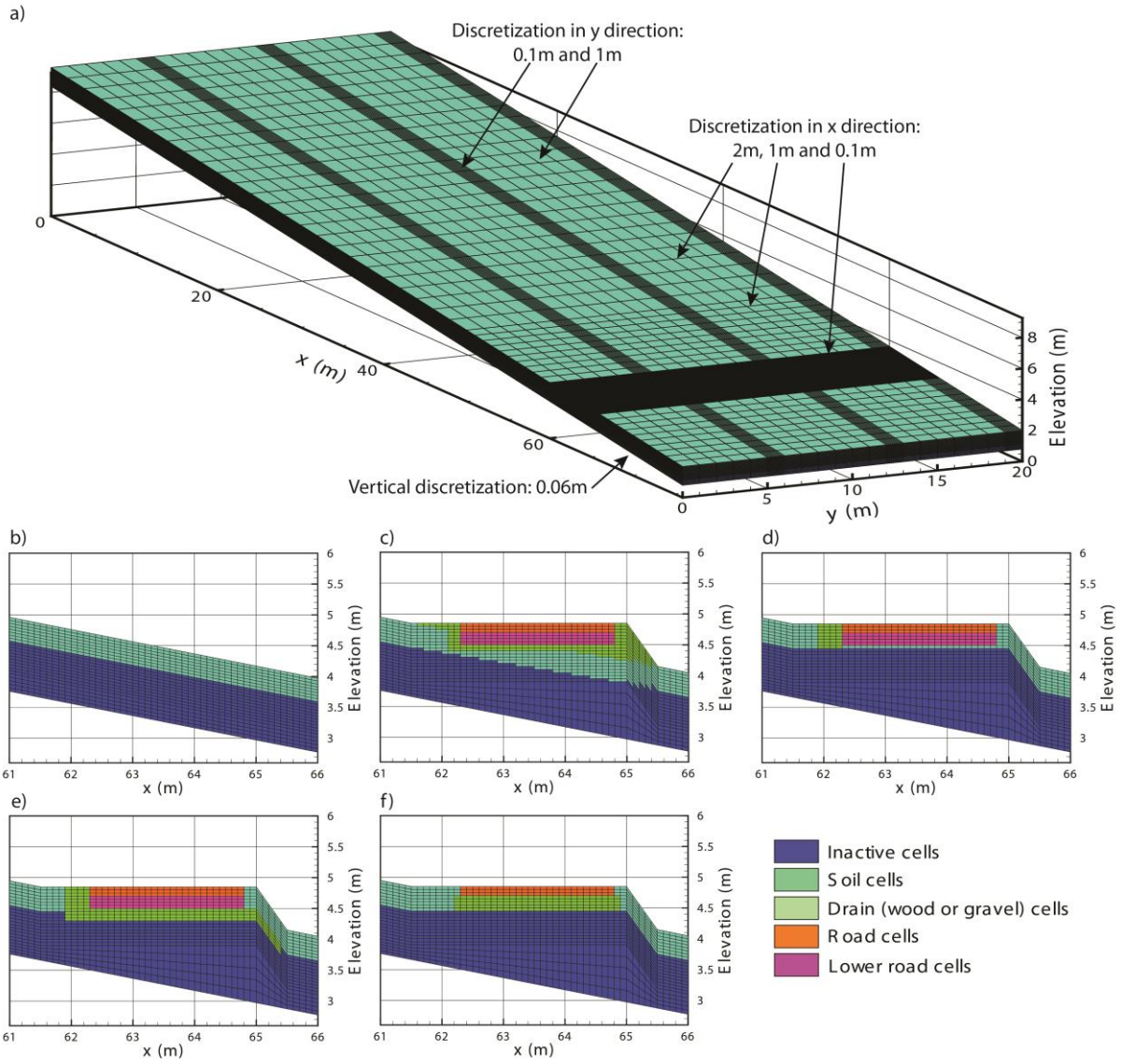

Figure 5 : Model development: a) Base case model, b) Base case model cross-section between 61m < x < 66m, c) No-excavation model between 61m < x < 66m, d) L-drain model between 61m < x < 66m, e) L-drain model between 61m < x < 66m along the transversal drain f) Wood-log model between 61m < x < 66m.

2.2.3 Model application

The model application consists of the variation of model properties to assess their effect on the groundwater dynamics. The following parameters were analyzed: fen slope, soil hydraulic conductivities and road drain hydraulic conductivities. These parameters were selected because according to the Darcy's law (1) they control the groundwater flow dynamics. K is the hydraulic conductivity of the soil and the drain and ∇H the hydraulic gradient of the fens which itself strongly influenced by the topographical slope.

$$q = K * \nabla H \quad (1)$$

For each property varied in the sensitivity analysis, three different values were chosen (Table 2): a low, intermediate and high value. For the soil hydraulic conductivities (KS), values presented in Charman (2002) were used and varied between 8.64m/d and 0.0864m/d. This corresponds to a soil composed of gravely organic matter (as observed for example in St-Antonien site) or loamy organic matter (as observed for example in Schoeniseischwand site). Van Genuchten parameters (α and β), as well as the residual water content, were not varied. The road drains (KD) which are made of coarse or very coarse gravel were assigned a hydraulic conductivity between 8640m/d and 86.4m/d (Fetter 2001), their van Genuchten parameters corresponding to gravel. The slopes were fixed at 10%, 20% and 30%, as observed during the fieldwork. The hydraulic conductivities of the wood-log (W-L) drain were assumed ten times more conductive and more porous than the gravel drain. The road concrete is almost impermeable and was thus conceptualized with a very low hydraulic conductivity, its van Genuchten parameters corresponding to fine material. The road basement is constructed using highly compacted fine material (sand and loam) and was thus implemented with low hydraulic conductivity, the van Genuchten parameters corresponding to fine material. Finally, the implemented soil and road surface flow properties correspond to a wetland and urban cover (Li et al., 2008).

Table 2 : Subsurface and surface flow parameters.

Subsurface flow properties

	Hydraulic conductivity	Porosity	Van Genuchten α	Van Genuchten β	Residual water content
Units	**K [md^{-1}]**	**θ [-]**	**α [m^{-1}]**	**β [-]**	**Swr [-]**
Soil - KS1	8.64	0.25	4	1.41	0.04
Soil - KS2	0.864	0.25	4	1.41	0.04
Soil - KS3	0.0864	0.25	4	1.41	0.04
Drains - KD1	8640	0.25	29.4	3.281	0.04
Drains - KD2	864	0.25	29.4	3.281	0.04
Drains - KD3	86.4	0.25	29.4	3.281	0.04
Drains - WL - KD1	86400	0.7	29.4	3.281	0.04
Drains - WL - KD2	8640	0.7	29.4	3.281	0.04
Drains - WL - KD3	864	0.7	29.4	3.281	0.04
Road concrete	0.0000864	0.05	1.581	1.416	0.04
Road basement	0.00864	0.25	4	1.416	0.04

Surface flow properties

	Coupling length	Manning's roughness coefficient		Rill storage height	Obstruction height
Units	**l_c [m]**	**n_x [$m^{-1/3}s$]**	**n_y [$m^{-1/3}s$]**	**D_t [m]**	**O_t [m]**
Soil	1. x 10^{-2}	0.03	0.03	0.005	0.005
Road	1. x 10^{-2}	0.018	0.018	0.001	0.001

In order to simulate each parameter combination, a total of 90 models were developed (27 models for each road structures and 9 models for natural conditions). Models are run for 10'000 days (about 27 years) with a constant flux equal to 380mm/y on the top representing the rainfall to reach a steady state. Subsequently, subsurface flow rates in the soil layer were extracted at each section with an area of 0.4m^2 (1m wide times the soil thickness) presented in Figure 6. Changes in subsurface flow rates indicate a perturbation of flow dynamics and therefore, a comparison of flow rates between each model was made to present the effect of each road structure and sloping fen properties on the dynamics.

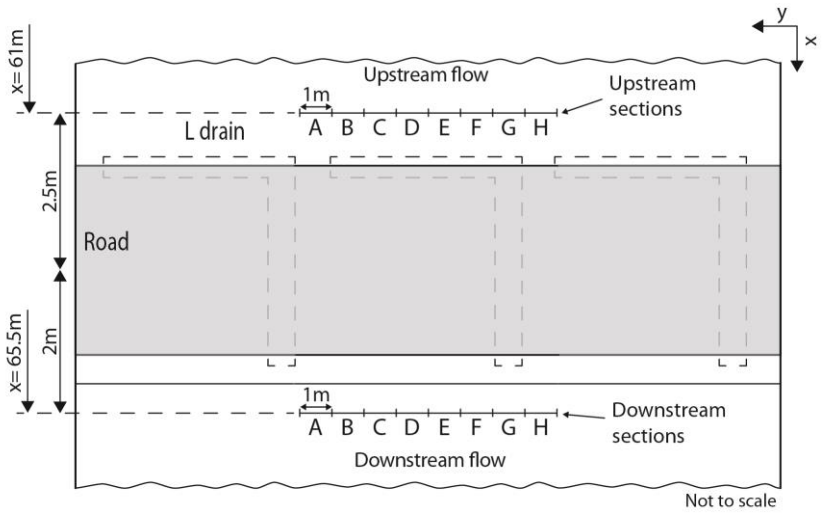

Figure 6 : Location of observation sections in the models.

3 Results and Discussion

3.1 Fieldwork

Based on the observations, all sites show a continuous saturated zone before the experiment, both upslope and downslope of the road, the hydraulic gradients being similar to the terrain slope (Figure 7, 1st column). In contrast, the EC maps established prior to the tracer test show a spatial variability of one to several meters (Figure 7, 2nd column.). Within each plot, EC varies from 482 to 629µS/cm. At the SCH site, the highest values are located downslope of the L-drain outlet which could indicate that the EC increases as water is flowing through the drain (e.g. through the dissolution of the construction material). Given that this initial distribution of EC is not uniform, the comparison of EC after the sprinkling experiment has to be made in a relative manner (Figure 7, 3rd column).

The heterogeneity of the hydraulic conductivity of the soil is apparent from the tracer tests (Figure 7, 3rd column: EC 24 hours after injection). At all four sites, the front of the saline solution is not uniform because of the heterogeneity of the soil hydraulic conductivity. Nevertheless, the road structures or the drains may create

preferential flow paths. This is clearly occurring at the SCH site where the front follows two preferential flow paths. One related to the L-drain (right path) and the other on the left, unrelated to the L-drain, suggesting that the latter drains only a part of the water and the other part follows a natural preferential flow path. At the HMD site, the saline solution is far more concentrated on the left side of the plot, yet apparently not as a result of the road's structure. Rather, the soil appears more permeable on the left side of the plot, both upslope and downslope of the road. Finally, the decrease in EC observed 24 hours after injection at some locations might result from the following: (1) the tracer injection induces, by "piston effect", the displacement of a small volume of local water with a lower EC; (2) the tracer injection was preceded by a period of irrigation without tracer. This could have diluted the pre-irrigation soil solution.

In each case, the irrigation experiments demonstrate the continuity of subsurface flow under the road for all structures. For the no-excavation and wood-log type, the perturbation of the flow field seems to be controlled by the natural heterogeneity of the soil and flow paths, and not by the road itself. Conversely, the field data strongly suggest that the L-drain constitutes an important preferential pathway and consequently subsurface flow is increasingly concentrated. This flow convergence can cause gully erosion.

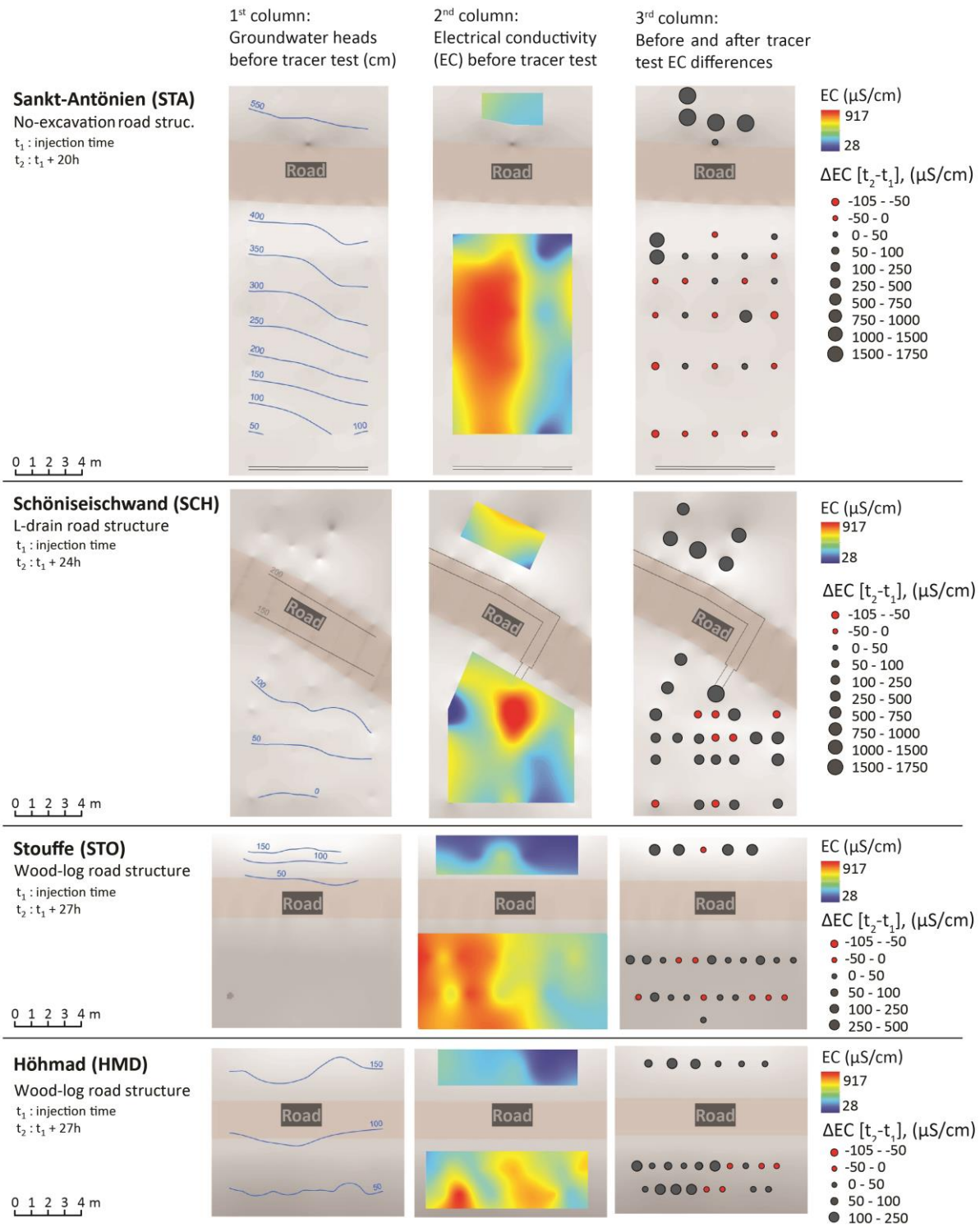

Figure 7 : Fieldwork results at the four field sites: 1st column) Measured groundwater heads before tracer test, 2nd column) measured EC before tracer test and 3rd before and after tracer test differences in EC. The hydraulic heads downslope the road in the Stouffe site is about 25cm and upslope the road in the Schöniseischwand is about 225cm (between two isolines) and are not presented in the figure

3.2 Modelling

Figure 8a shows the results of the models with a slope of 10%, Figure 8b with a slope of 20% and Figure 8b with a slope of 30%. In each dot chart, the groundwater flow rates (always in m^3/d) are plotted with crosses for the base case model, diamonds for the no-excavation type, squares for the L-drain type and circles for the wood-log type. In addition, the maximum flow rate capacity of the soil calculated with Darcy's Law (1) and the flow rate induced by the precipitation are also presented for the interpretation of the results. In the following paragraphs, the base case (natural conditions) results are presented and discussed, followed by the simulations of the road structures.

In the base case model, groundwater flow rates vary from 0.003 (m^3/d) to 0.069 (m^3/d) for a 10% slope, 0.006 (m^3/d) to 0.069 (m^3/d) for a 20% slope and from 0.009 (m^3/d) to 0.069 (m^3/d) for a 30% slope. The groundwater flow rate decreases following a decrease of the hydraulic conductivities (KS) of the soil layer. The groundwater flow rates are mainly controlled by the hydraulic conductivities, the slope plays a less important role. This is expected, as the ratios of the maximum and minimum hydraulic conductivity are two orders of magnitude, while slopes were multiplied by a factor of two (for a slope of 20%) or three (for a slope of 30%). Therefore, groundwater flow is increased by a factor 3 between the model KS3 with a slope of 10% and model KS3 with a slope of 30%. Concerning the formation of surface flow the following observation can be made. For all KS2 and KS3 models, surface flow occurs while the infiltration capacity of the KS1 models is never exceeded and thus no surface flow occurs.

In the no-excavation and wood-log type models, the influence on flowrates caused by the presence of the road structures is quite similar. Groundwater flows vary from 0.01 (m^3/d) to 0.069 (m^3/d) for a 10% slope, 0.01 (m^3/d) to 0.069 (m^3/d) for a 20% slope and to 0.010 (m^3/d) to 0.069 (m^3/d) for a 30% slope. Compared to the base case model, results show that the no-excavation and wood-log type structures have a minimal impact on flow perturbation. The only marked difference is that groundwater flow rates are slightly higher if the soil hydraulic conductivities are low (KS3). This is due to the hydraulic conductivity of the base of the road (consisting of wood-logs) higher than the hydraulic conductivity of the soil which facilitates infiltration. Conversely, in the base case model, less water is infiltrated but more surface runoff occurs. In the 20% and 30% slope models, the results of the no-excavation model are similar to the base case model.

316 In the L-drain model, the effect of the road is markedly different from the other road structures. The
317 groundwater flows vary significantly in the observation sections. The maximum flows are always obtained in the
318 observation section G (see Figure 6 for the location of the sections) just downslope of the drain outlet and can be
319 10 times higher than compared to the base case. Conversely, minimum flows are obtained in observation sections
320 C and D in which flow rates can be 10 times lower. Significant differences in groundwater flow are also observed
321 in the same transect (within the same model). To condense this information, the ratios between maximum and
322 minimum flow rate are calculated for the L-drain structures (numbers at the bottom right of the panels in Figure
323 8). The maximum differences are observed for the cases where the hydraulic conductivity of soil (KS) and drain
324 (KD) are high and vary from 0.025 (m^3/d) to 0.150 (m^3/d). Conversely, when KS and/or KD are low, the
325 differences along the transect are smaller. Finally, the slope accentuates groundwater flow rate differences along
326 the transect. Therefore, an increase of groundwater flow differences is observed for the 10% and 30% slope
327 scenarios, within the same model. The impact of the L-drain may be further explored by extracting groundwater
328 flows lower than 2m downslope the road to assess the extent of perturbations. Figure 9 shows simulated
329 groundwater flows for the most critical cases (i.e. KS1 with a slope of 10%, 20% and 30%) downslope the road at
330 3.5m and 6.5m respectively and 2.5m upslope. At 3.5m the groundwater flows already regain their upslope
331 conditions. At 6.5m downslope the road, all observation sections are very close to the upslope flows except in
332 section G where flows are still slightly higher.

333 In addition to the assessment of perturbation through roads, the model results can be used to evaluate the
334 risk of gully erosion. As presented in Figure 8, the maximum flow rate capacity of the soil is small in comparison
335 to precipitation. For all model scenarios except for KS1, the soil capacity is lower than the precipitation and thus
336 surface runoff occurs in the models and is likely to occur naturally. However, surface runoff may be triggered by
337 the presence of L-drain structures. To illustrate this process, the simulated surface flow velocities of each road
338 structure downslope the road for the model KS2-KD2 and slope of 20% are presented in Figure 10. In this case,
339 the maximum flow rate capacity of the soil is approximately equal to precipitation, therefore runoff should not
340 occur. However, this is not the case for the L-drain. The occurrence of surface runoff is the consequence of the
341 subsurface flow concentration. In this configuration, the infiltration capacity of the soil is too small to
342 accommodate the concentrated flow collected upslope, thus groundwater emerges and surface flow is triggered.
343 This constitutes an increase of the risk for gully erosion. In addition, the perturbation on the roads upslope of the
344 road was assessed.

Finally, the impact of road structure on the upslope road dynamics was be also assessed (Figure not shown) 2.5m upslope. Upslope flows are similar to the base case model, thus the influence of the road is, not unexpectedly, marginal for all road types.

The development of models with various combinations of parameters allowed for exploring a larger parameter space than using field work only. For instance, the fact that the impact of an L-drain structure on the water dynamics is less marked if the hydraulic conductivity of soil is low would have been impossible to identify by using fieldwork only. However, a numerical model is always a simplified reproduction of reality. The main model assumption is that the hydraulic conductivity of the soil is homogeneous. However, the models are not intended to reproduce small-scale observations, i.e. the exact hydraulic head in a piezometer, but instead can be used to explore the influence of the road structures under different soil conditions (overall hydraulic conductivity) and slopes. Given that no horizontal redistribution of the flow downslope can be simulated, for this the consideration of heterogeneity would be required, consequently, the models constitute a worst-case scenario. The models allow for a relative ranking of the potential impact and clearly show the increased risk for surface water flow generation and thus gully erosion. Clearly, the L-drain shows the largest impact. The two other road structures are thus the preferred choice.

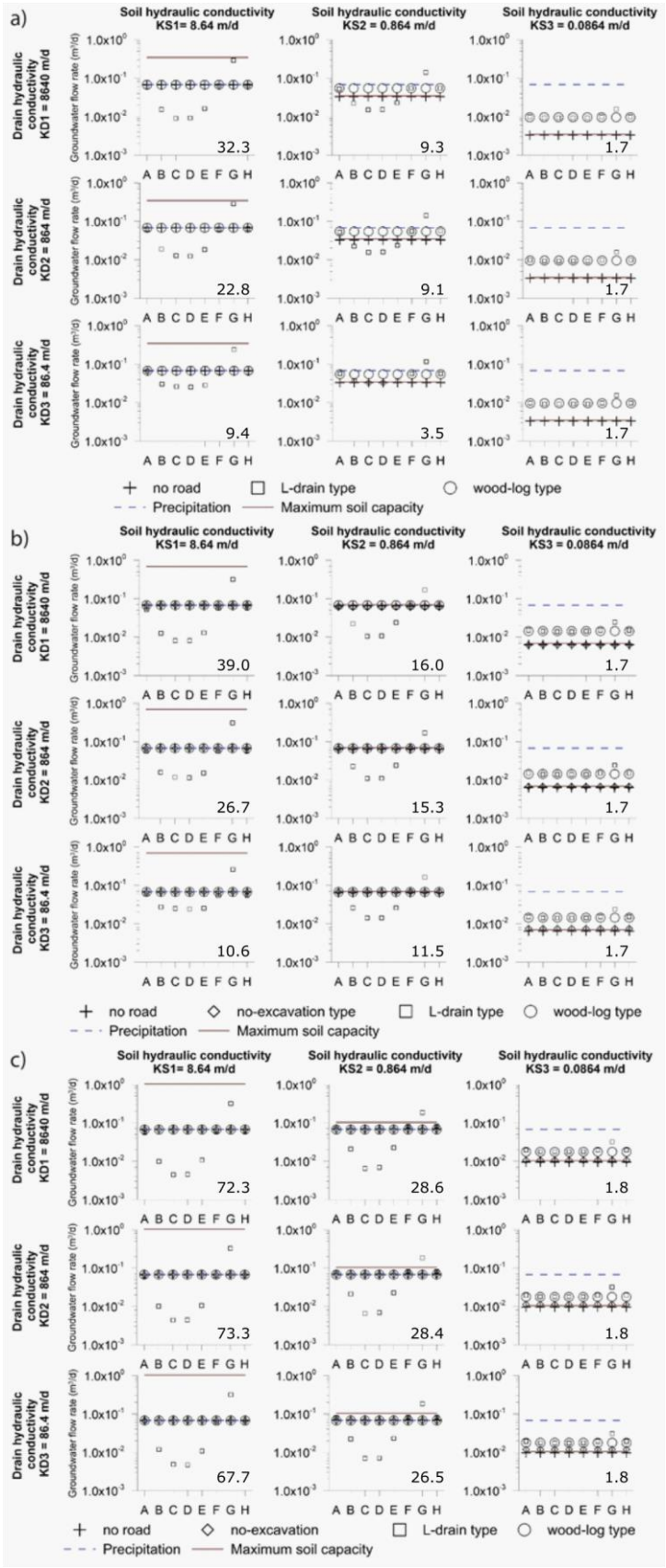

362

363 **Figure 8 : Simulated groundwater flow rates 2m downslope each road structure and each parameter combination**
364 **with a slope of a) 10%, b) 20% and c) 30%. Numbers at the bottom right of each panel are the ratio between**
365 **maximum and minimum groundwater flow within the L-drain transect**

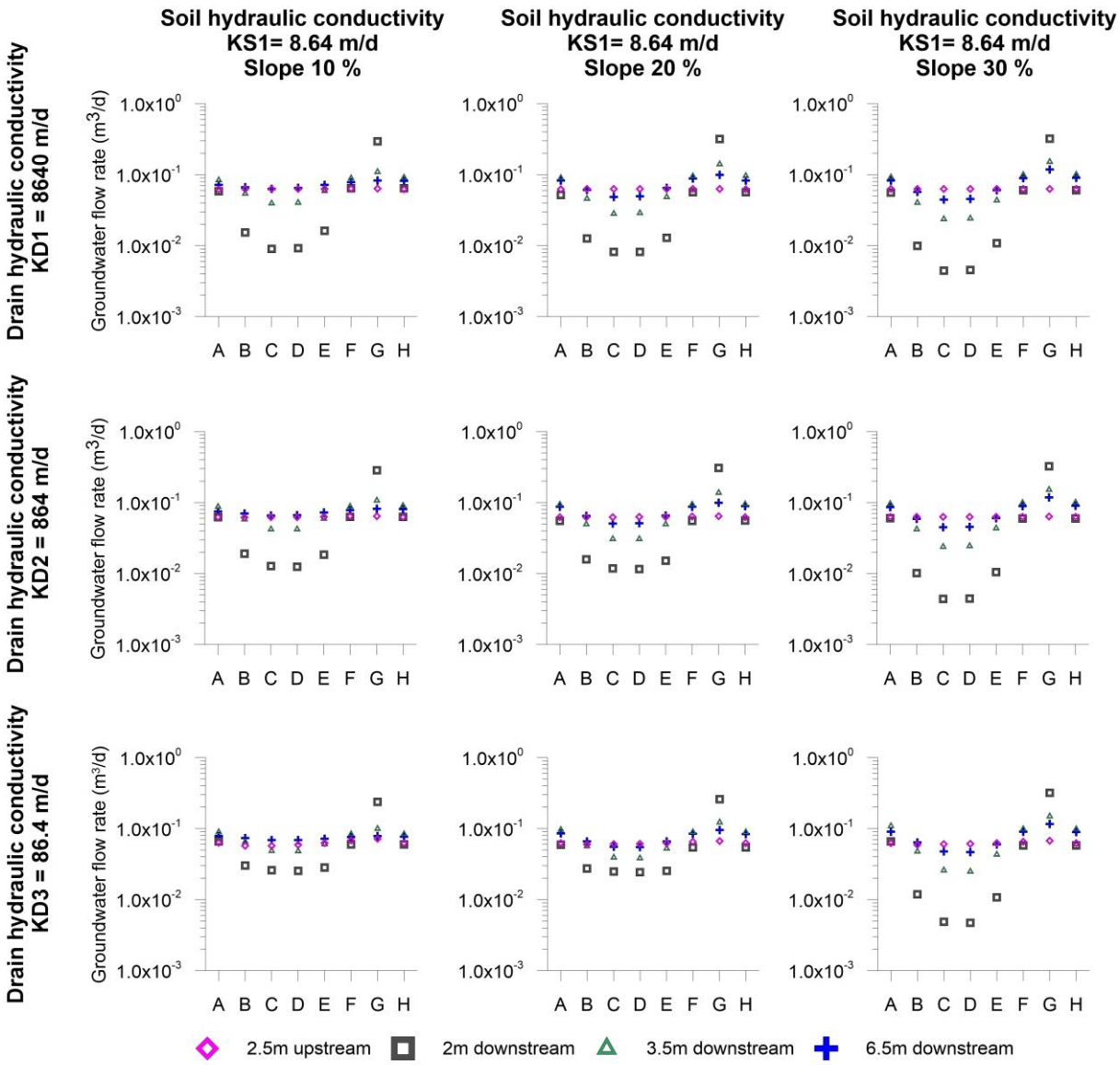

Figure 9 : Extent of perturbations due to the L-drain road type: Simulated groundwater flow rates different distances the road.

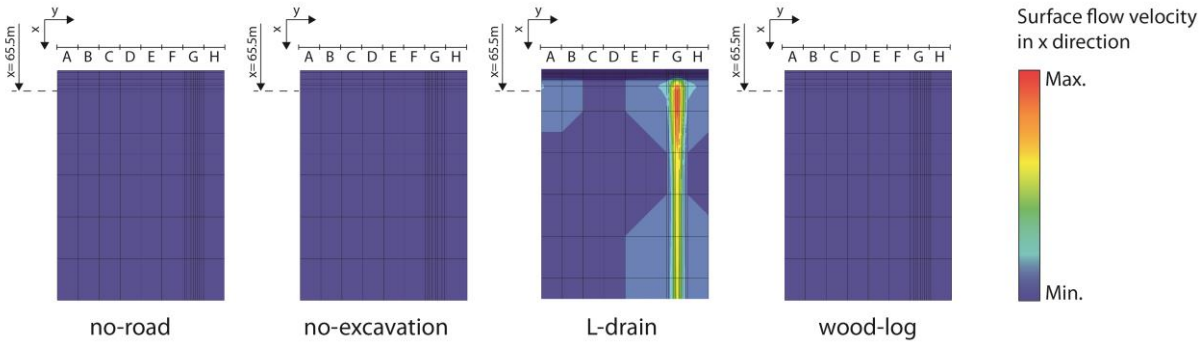

Figure 10 : Simulated surface flow of the KS2-KD2 model and a slope of 20% for each road structure. The results clearly indicate the increased risk caused by the L-drain of triggering surface runoff and thus potentially gully-erosion and the drying out of sections of the wetland

4 Conclusions

This study assessed three road structures regarding their perturbations of the natural groundwater flow. Two of these road structures were specifically developed to reduce the negative impacts of the road. The study is based on two complementary approaches; field-based tracer tests and numerical models simulating groundwater flow for the different road structures. The combination of fieldwork and the development of numerical models was fundamental to achieve the goal of this study. The tracer test allowed for a better understanding of groundwater flow throughout road structures and allowed for evaluating their effectiveness at a given location. However, the tracer tests are time-consuming and only a few field sites are available. The numerical approach, on the other hand, allows for exploring any combination of slope, hydraulic properties or road structure, thus providing a more comprehensive approach. The significant impact of the L-drain road structure is clearly established in the numerical approach and is consistent with the field observations. For the other road structures too, the numerical models are consistent with fieldwork results by showing relatively undisturbed groundwater flow downslope the road.

It is the first time that the performance of these road-structures has been investigated in the field. The tracer tests showed that both sides of the road where hydraulically connected for all investigated road structures. Groundwater flow was heterogeneous suggesting the occurrence of natural preferential flow paths in the soil. The presence of a transversal drain (L-drain) beneath the road suggests that an L-drain constitutes a preferential flow path of much greater importance than the naturally occurring preferential pathways. The field results further suggest that the wood-log and no-excavation structures as less impactful that the L-drain. The simulation results are consistent with the assessment of the relative impact of the different road-types. Groundwater flow rates 10 times larger than in the natural case were obtained in the numerical simulations. The two other road structures

(wood-log and no-excavation) do not perturb the flow field to the extent of the L-drain. To minimize the perturbation of flow fields, the wood-log and no-excavation structures are recommended.

5 Acknowledgements

This research was funded by the Swiss Federal Office for the Environment (FOEN) and supported by the Swiss Federal Office for Agriculture (FOAG). The authors are grateful to Benoit Magnin, Peter Staubli Andreas Stalder, Anton Stübi and Ueli Salvisberger for their collaborations. We thank the three anonymous reviewers and the editor for their constructive comments. We thank the three anonymous reviewers and the Editor, A: Hildebrandt, for their input to the paper.

6 References

Baker, C., Thompson, J. R. and Simpson. M.: 6. Hydrological Dynamics I: Surface Waters, Flood and Sediment Dynamics The Wetlands Handbook, 1st edition. Edited by E. Maltby and T. Barker. 2009. Blackwell Publishing, 120-168, 2009.

Betts, H. D., and DeRose, R. C.: Digital elevation models as a tool for monitoring and measuring gully erosion, International Journal of Applied Earth Observation and Geoinformation, 1, 91-101, http://dx.doi.org/10.1016/S0303-2434(99)85002-8, 1999.

Broggi, M. E.: Minimum requis de surfaces proches de l'état naturel dans le paysage rural, illustré par l'exemple du Plateau suisse. Liebefeld-Berne., Rapport 31a du Programme national de recherche "Sol", 199p, 1990.

Brunner, P., and Simmons, C. T.: HydroGeoSphere: a fully integrated, physically based hydrological model, Groundwater, 50, 170-176, 2012.

Capra, A., Porto, P., and Scicolone, B.: Relationships between rainfall characteristics and ephemeral gully erosion in a cultivated catchment in Sicily (Italy), Soil and Tillage Research, 105, 77-87, http://dx.doi.org/10.1016/j.still.2009.05.009, 2009.

Charman, D.: Peatlands and environmental change. John Wiley & Sons Ltd. 301 2002.

Chimner, R. A., Cooper, D. J., Wurster, F. C. and Rochefort, L.: An overview of peatland restoration in North America: where are we after 25 years?, Restoration Ecology, 25, 283-292, 2016.

Cochand, F., Therrien, R., and Lemieux, J.-M.: Integrated Hydrological Modeling of Climate Change Impacts in a Snow-Influenced Catchment, Groundwater, 57, 3-20, doi:10.1111/gwat.12848, 2019.

Cognard Plancq, A. L., Bogner, C., Marc, V., Lavabre, J., Martin, C., and Didon Lescot, J. F.: Etude du rôle hydrologique d'une tourbière de montagne: modélisation comparée de couples "averse-crue" sur deux bassins versants du Mont-Lozère., Etudes de géographie physique, n° XXXI, p. 3 - 15, 2004.

Daba, S., Rieger, W., and Strauss, P.: Assessment of gully erosion in eastern Ethiopia using photogrammetric techniques, CATENA, 50, 273-291, http://dx.doi.org/10.1016/S0341-8162(02)00135-2, 2003.

Derose, R. C., Gomez, B., Marden, M., and Trustrum, N. A.: Gully erosion in Mangatu Forest, New Zealand, estimated from digital elevation models, Earth Surface Processes and Landforms, 23, 1045-1053, 10.1002/(SICI)1096-9837(1998110)23:11<1045::AID-ESP920>3.0.CO;2-T, 1998.

Descroix, L., González Barrios, J. L., Viramontes, D., Poulenard, J., Anaya, E., Esteves, M., and Estrada, J.: Gully and sheet erosion on subtropical mountain slopes: Their respective roles and the scale effect, CATENA, 72, 325-339, http://dx.doi.org/10.1016/j.catena.2007.07.003, 2008.

Dutton, A. L., Loague, K., and Wemple, B. C.: Simulated effect of a forest road on near-surface hydrologic response and slope stability, Earth Surface Processes and Landforms, 30, 325-338, 10.1002/esp.1144, 2005.

Li, Q., Unger, A. J. A., Sudicky, E. A., Kassenaar, D., Wexler, E. J., and Shikaze, S.: Simulating the multi-seasonal response of a large-scale watershed with a 3D physically-based hydrologic model, Journal of Hydrology, 357, 317-336, http://dx.doi.org/10.1016/j.jhydrol.2008.05.024, 2008.

Limpens, J., Berendse, F., Blodau, C., Canadell, J. G., Freeman, C., Holden, J., Roulet, N., Rydin, H. and Schaepman-Strub, G.: Peatlands and the carbon cycle: from local processes to global implications – a synthesis, Biogeosciences, 5, 1475-1491, 2008.

Lindsay, R.: Peatbogs and carbon: a critical synthesis to inform policy development in oceanic peat bog conservation and restoration in the context of climate change, University of East London, Technical Report, 2010.

Loague, K., and VanderKwaak, J. E.: Simulating hydrological response for the R-5 catchment: comparison of two models and the impact of the roads, Hydrological Processes, 16, 1015-1032, 10.1002/hyp.316, 2002.

Martínez-Casasnovas, J. A.: A spatial information technology approach for the mapping and quantification of gully erosion, CATENA, 50, 293-308, http://dx.doi.org/10.1016/S0341-8162(02)00134-0, 2003.

Nyssen, J., Poesen, J., Moeyersons, J., Luyten, E., Veyret-Picot, M., Deckers, J., Haile, M., and Govers, G.: Impact of road building on gully erosion risk: a case study from the Northern Ethiopian Highlands, Earth Surface Processes and Landforms, 27, 1267-1283, 10.1002/esp.404, 2002.

Partington, D., Therrien, R., Simmons, C. T., and Brunner, P.: Blueprint for a coupled model of sedimentology, hydrology, and hydrogeology in streambeds, Reviews of Geophysics, 55, 287-309, 10.1002/2016rg000530, 2017.

Poesen, J., Nachtergaele, J., Verstraeten, G., and Valentin, C.: Gully erosion and environmental change: importance and research needs, CATENA, 50, 91-133, http://dx.doi.org/10.1016/S0341-8162(02)00143-1, 2003.

Reckendorfer, W., Funk, A., Gschöpf, C., Hein, T. and Schiemer, F.: Aquatic ecosystem functions of an isolated floodplain and their implications for flood retention and management, Journal of Applied Ecology , 50, 119–128, 2013.

Reid, L. M., and Dunne, T.: Sediment production from forest road surfaces, Water Resources Research, 20, 1753-1761, 10.1029/WR020i011p01753, 1984.

Rydin, H. a. J., J.: The biology of peatlands, Oxford University Press, 343p., 2005.

Samaritani, E., Siegenthaler, A., Yli-Petäys, M., Buttler, A., Christin, P.-A., and Mitchell, E. A. D.: Seasonal Net Ecosystem Carbon Exchange of a Regenerating Cutaway Bog: How Long Does it Take to Restore the C-Sequestration Function?, Restoration Ecology, 19, 480-489, 10.1111/j.1526-100X.2010.00662.x, 2011.

Valentin, C., Poesen, J., and Li, Y.: Gully erosion: Impacts, factors and control, CATENA, 63, 132-153, http://dx.doi.org/10.1016/j.catena.2005.06.001, 2005.

Van Genuchten, M. T.: A closed-form equation for predicting the hydraulic conductivity of unsaturated soils, Soil science society of America journal, 44, 892-898, 1980.

VanderKwaak, J. E.: Numerical simulation of flow and chemical transport in integrated surface-subsurface hydrologic systems, Ph.D. thesis, Departement of Earth Science, University of Waterloo, Waterloo, Ontario, Canada., 1999.

Von Sengbusch, P.: Enhanced sensitivity of a mountain bog to climate change as a delayed effect of road construction, Mires and Peat, 15: Art. 6, (Online: http://www.mires-and-peat.net/pages/volumes/map15/map1506.php), 2015.

Wemple, B. C., and Jones, J. A.: Runoff production on forest roads in a steep, mountain catchment, Water Resources Research, 39, 2003.

Zollner, A.: Das Abflussgeschehen von unterschiedlich genutzten Hochmooreinzugsgebieten - Bayer. Akad. f. Naturschutz u. Landschaftspflege - Laufen / Salzach, Laufener Seminarbeitr. , 111-119, 2003.